

## ON CRACK PATH SELECTION AND THE INTERFACE FRACTURE ENERGY IN BIMATERIAL SYSTEMS

A. G. EVANS<sup>1</sup>, B. J. DALGLEISH<sup>1</sup>, M. HE<sup>1</sup> and J. W. HUTCHINSON<sup>2</sup>

<sup>1</sup>Materials Department, College of Engineering, University of California, Santa Barbara, CA 93106 and

<sup>2</sup>Division of Applied Sciences, Harvard University, Cambridge, MA 02138, U.S.A.

(Received 10 May 1989)

**Abstract**—The intent of this article is to apply recent solutions for the mechanics of cracks at and near bimaterial interfaces to rationalize crack trajectories observed by experiment and to provide a basis for interpreting measurements of the interface fracture energy,  $\Gamma_i$ . It is demonstrated that the choice of test specimen governs the tendency of cracks to either remain at interfaces or deviate away, based on considerations of the phase angle of loading,  $\psi$ . It is further revealed that the measured interface fracture energy may be strongly influenced by the crack trajectory, as governed by  $\psi$ , through crack shielding and plasticity effects. Consequently, interfaces do not typically have unique fracture energies, but instead  $\Gamma_i$  depends on  $\psi$  which, in turn, is influenced by the test method.

**Résumé**—Le but de cet article est d'appliquer des solutions récentes à l'étude de mécanisme des fissures sur et près des interfaces entre deux matériaux afin de rationaliser les trajectoires des fissures observées expérimentalement et de fournir une base à l'interprétation des mesures de l'énergie de fracture d'interface  $\Gamma_i$ . On démontre que le choix du type d'essai gouverne la tendance des fissures soit à rester aux interfaces soit à s'en écarter, suivant le déphasage de charge  $\psi$ . De plus on montre que l'énergie de rupture d'interface mesurée peut être fortement influencée par la trajectoire de la fissure, gouvernée par  $\psi$ , malgré l'écrantage des fissures et les effets de plasticité. En conséquence, les interfaces n'ont pas typiquement des énergies de rupture uniques, mais en revanche  $\Gamma_i$  dépend de  $\psi$  qui, à son tour, est influencé par la méthode d'essai.

**Zusammenfassung**—In dieser Arbeit sollen kürzlich erhaltene Lösungen für die Rißmechanik von Rissen an den und in der Nähe der Grenzflächen zwischen zwei Materialien angewendet werden auf die experimentell beobachteten Trajektorien der Risse, um so eine Grundlage für die Deutung der Messungen der Bruchenergie an der Grenzfläche  $\Gamma_i$  zu erhalten. Es wird dargelegt, daß die Wahl der Proben die Tendenz der Risse bestimmt, entweder an der Grenzfläche zu bleiben oder davon abzuweichen; hierzu wird der Phasenwinkel  $\psi$  der Belastung betrachtet. Außerdem wird gezeigt, daß die gemessene Energie für den Bruch an der Grenzfläche von der Rißtrajektorie stark beeinflusst werden kann, da sie von  $\psi$  über Rißabschirmung und plastische Effekte bestimmt ist. Folglich haben die Energien für Bruch an der Grenzfläche üblicherweise keine einheitlichen Werte, sondern  $\Gamma_i$  hängt von  $\psi$  ab, welches seinerseits von der Prüfmethode beeinflusst wird.

### 1. INTRODUCTION

Fracture along and adjacent to bimaterial interfaces has several morphological manifestations. In some cases, the fracture occurs at the interface, while in others fracture occurs in the more brittle constituent [1, 2]. Furthermore, cases exist wherein the fracture alternates between the interface and the adjacent material (Fig. 1) and in other instances, the crack deviates from one interface to the other [1, 4] (Fig. 2). The path selected by the crack also influences the fracture energy. In particular, fracture energies  $\Gamma_i$  have been measured for "interface" cracks wherein  $\Gamma_i$  has substantially exceeded that for the brittle constituent,  $\Gamma_s$  [4–6]. This behavior is seemingly at variance with intuitive reasoning that cracks should propagate in the "material" having the lowest

fracture energy. The present article constitutes an attempt to rationalize these features of interface fracture by invoking recent mechanics solutions for cracks at and near interfaces [7].

### 2. CRACK TRAJECTORIES

Various hypotheses have been made concerning crack trajectories in homogeneous brittle solids. Experiments that exhibit sensitivity to the choice of crack path criterion involve the decohesion of thin films from brittle substrates [8–10], particularly the location of the steady-state crack path within the substrate [11] (Fig. 3). The experimental results are consistent with the postulate that the crack acquires a trajectory in which the mode II stress intensity factor,  $K_{II}$ , is zero. A corollary of this criterion is that

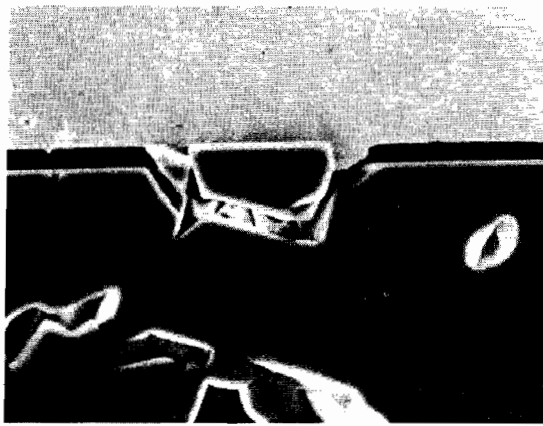


Fig. 1. Fracture of a Au/Al<sub>2</sub>O<sub>3</sub> bond indicating fragment of Al<sub>2</sub>O<sub>3</sub> attached to Au.

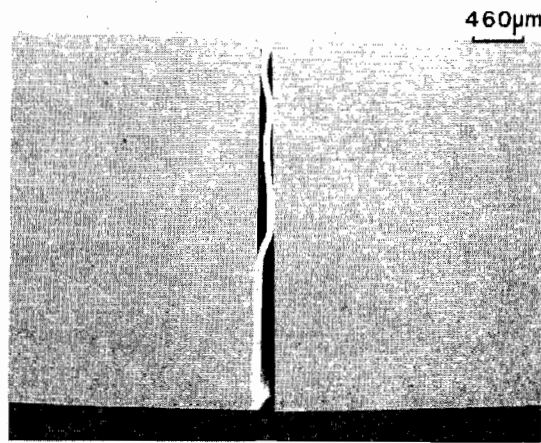


Fig. 2. A crack in Al<sub>2</sub>O<sub>3</sub> bonded with Au showing a crack alternating between interfaces.

a crack cannot remain in a plane having non-zero  $K_{II}$ , but instead is deflected in a direction that reduces  $K_{II}$  toward zero.

The above crack path criterion clearly does not apply when the crack is at an interface, because consideration of the relative fracture energy,  $\Gamma_i/\Gamma_s$ , is also involved. Analysis of the kinking of a crack out of an interface between two brittle solids [7] has revealed that the crack path depends both on  $\Gamma_i/\Gamma_s$  and the relative shear  $v$  to opening,  $u$ , experienced by the interface crack, as characterized by the phase angle  $\psi$  [12]

$$\psi = \tan^{-1}(v/u) - \epsilon \ln r - \tan^{-1} 2\epsilon \quad (1a)$$

where

$$\epsilon = \frac{1}{2\pi} \ln \left( \frac{1-\beta}{1+\beta} \right) \quad (1b)$$

with the Dundurs' parameters,  $\alpha$  and  $\beta$ , given by

$$\alpha = \frac{\mu_1(1-\nu_2) - \mu_2(1-\nu_1)}{[\mu_1(1-\nu_2) + \mu_2(1-\nu_1)]} \quad (1c)$$

$$\beta = \frac{\mu_1(1-2\nu_2) - \mu_2(1-2\nu_1)}{2[\mu_1(1-\nu_2) + \mu_2(1-\nu_1)]}$$

and  $r$  is the distance from the crack tip. Note that, for  $\beta = 0$  (typical of many systems of interest)

$$\psi = \tan^{-1}(v/u) \equiv \tan^{-1}(K_{II}/K_I) \quad (2)$$

and thus  $\psi$  is a direct measure of the relative mode II loading on the interface crack. Trends in the incidence of kinking out of the interface with  $\Gamma_i/\Gamma_s$  and  $\psi$  are shown in Fig. 4, for the range in  $\alpha$  of practical interest.

The solutions of Fig. 4 may be interpreted by equating  $\Gamma_s$  to the fracture energy of material 2 such that the sign  $\alpha$  is consistent with equation (1c). It is apparent that the preferred path of the crack is influenced by the magnitude of the phase angle, such that cracking out of the interface is most likely when  $\psi = 70^\circ$  and, furthermore, that the crack prefers to

extend into lower modulus material (subject to  $\psi$  having the appropriate sign, i.e. material 2 in Fig. 4 being the lower modulus member).

A related problem of substantial importance concerns the case wherein one of the materials is ductile and the other is brittle. Then the fracture behavior and the "interface" fracture energy are extremely sensitive to the sign of the phase angle. Some of the basic behaviors are summarized in Fig. 5. When the phase angle has a positive sign, in accordance with the sign convention given in Fig. 5, and material  $S$  is the brittle member (such that  $\Gamma_s \ll \Gamma_f$ ), the relative incidence of cracking out of the interface is identical to that described for the all-brittle system (Fig. 4). However, when the phase angle is negative, the large fracture energy of material  $F$ , compared with the interface ( $\Gamma_f \gg \Gamma_i$ ) prohibits propagation of the crack out of the interface. Then, one of two possibilities occurs, depending upon the yield strength of the ductile member. For a low yield strength material, plastic blunting of the interface crack is observed [Fig. 6(a)] and failure often occurs by ductile mechanisms [Fig. 6(b)] involving hole nucleation at the

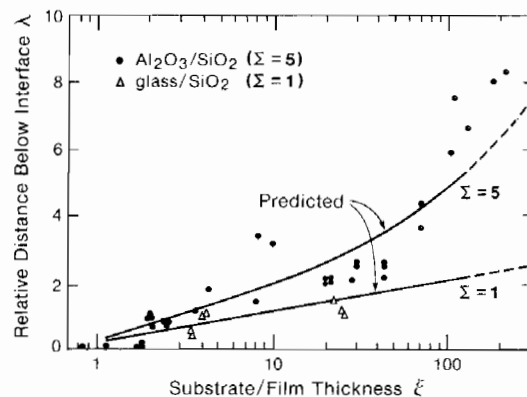


Fig. 3. Film decohesion by substrate cracking indicating the predicted crack location based on  $K_{II} = 0$  and experimental data obtained for two material combinations.

3. THE INTERFACE FRACTURE ENERGY

The above discussion concerning crack paths has important implications for measuring and interpreting information relating to the “fracture energy of interfaces”. Most importantly, the test configuration determines the sign and the magnitude of  $\psi$ , which in turn governs the crack path and thus, the mechanisms that contribute to  $\Gamma_i$ . Several examples are used to illustrate the salient features: “mode I” sandwich specimens [4, 13] [Fig. 7(a)], peel tests [5] [Fig. 7(b)] and film decohesion tests [14] [Fig. 7(c)]. In all cases, residual stress contributes substantially to the observed behavior and in the interpretation of the results.

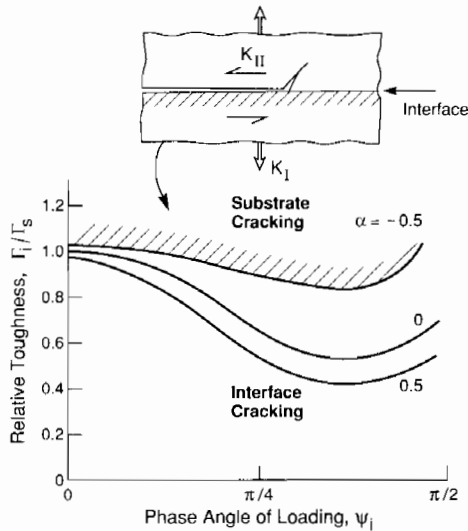


Fig. 4. A map representing the region of interface cracking for three values of the elastic mismatch parameter  $\alpha$ . Positive  $\psi$  is defined by the mode II arrows in the inset diagram.

interface [3]. Alternatively, the stress field of the interface crack interacts with preexisting flaws in the brittle material, causing cracks to grow from these flaws back toward the interface, resulting in a serrated fracture with “chips” of brittle material attached to the fracture surface (Figs 1 and 5). This behavior can be understood by noting that the flaws in the brittle material are subject to substantial mode II loading having sign that leads to crack extension toward the interface.

3.1. Sandwich tests

The interpretation of fracture tests performed on sandwich specimens is relatively straightforward when the precrack length,  $a$ , is very large compared with the bond layer thickness,  $h$  ( $a \geq 30h$ ). Then, the residual strain does not contribute to the energy release rate  $G$ , because the bond layer remains attached to one side of the specimen and thus, retains its state of residual strain [15]. When this crack length condition is satisfied, the only other significant consideration is the influence of the bond layer on the magnitude of  $G$  and  $\psi$ . When  $h$  is small compared with the specimen thickness,  $d$ , the energy release rate is unaffected by the layer [13]. However, the presence of the layer causes  $\psi$  to deviate from zero. For the typical case,  $\beta \approx 0$ ,  $\psi$  is governed solely by  $\alpha$ , with the trend [13] plotted on Fig. 8. While the range in  $\psi$  is small, it is often sufficient to influence the crack trajectory. Specifically, in most cases, the shear modulus of the bond layer is less than that of the bonded member, whereupon the sign of  $\psi$  directs the crack toward the interface. Consequently, when the bond material is ductile, the crack tends to either remain at the interface or follow a serrated path near the interface. In either case, plasticity in the bond layer can contribute to  $\Gamma_i$ , causing the measured fracture energy to be substantially greater than  $\Gamma_s$  even though the crack remains near the interface.

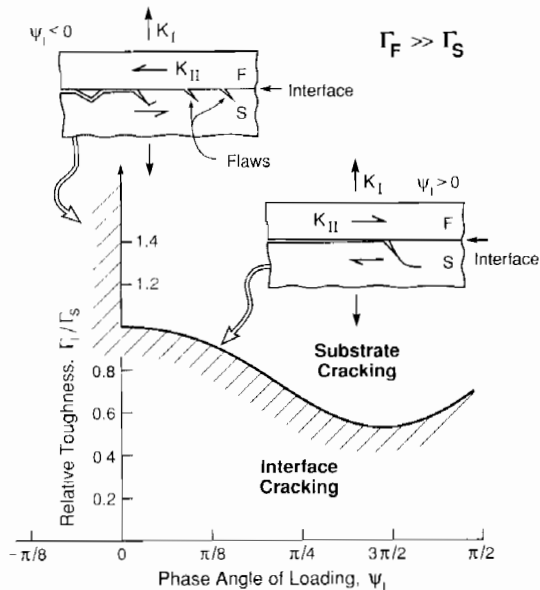


Fig. 5. The region of interface fracture for a bimaterial system when one material,  $F$ , has a much higher fracture energy than the other,  $S$  ( $\Gamma_F \gg \Gamma_S$ ). The result is plotted for the case,  $\alpha = \beta = 0$ . Note that when  $\psi < 0$ , fracture at the interface can incorporate segments of adjoining material detached at flaws.

When the crack is not long compared with the layer thickness, residual stress influences both  $K_I$  and  $K_{II}$  and must be taken into account [15]. Most significantly, when the bond layer has the larger thermal expansion coefficient, the sign of  $\psi$  tends to divert the crack away from the interface and furthermore, is sufficiently large ( $\psi \approx 45^\circ$ ) [15] that it can dominate the overall phase angle at the fracture criticality. In this case, cracks are often diverted into the brittle material, outside the bond [2]. The nominal fracture energy measured in such cases can have a broad range of values that depend on the crack length and the residual strain [16]. However, the actual fracture energy can be deduced if the residual strain contribution to  $G$  is properly taken into account.

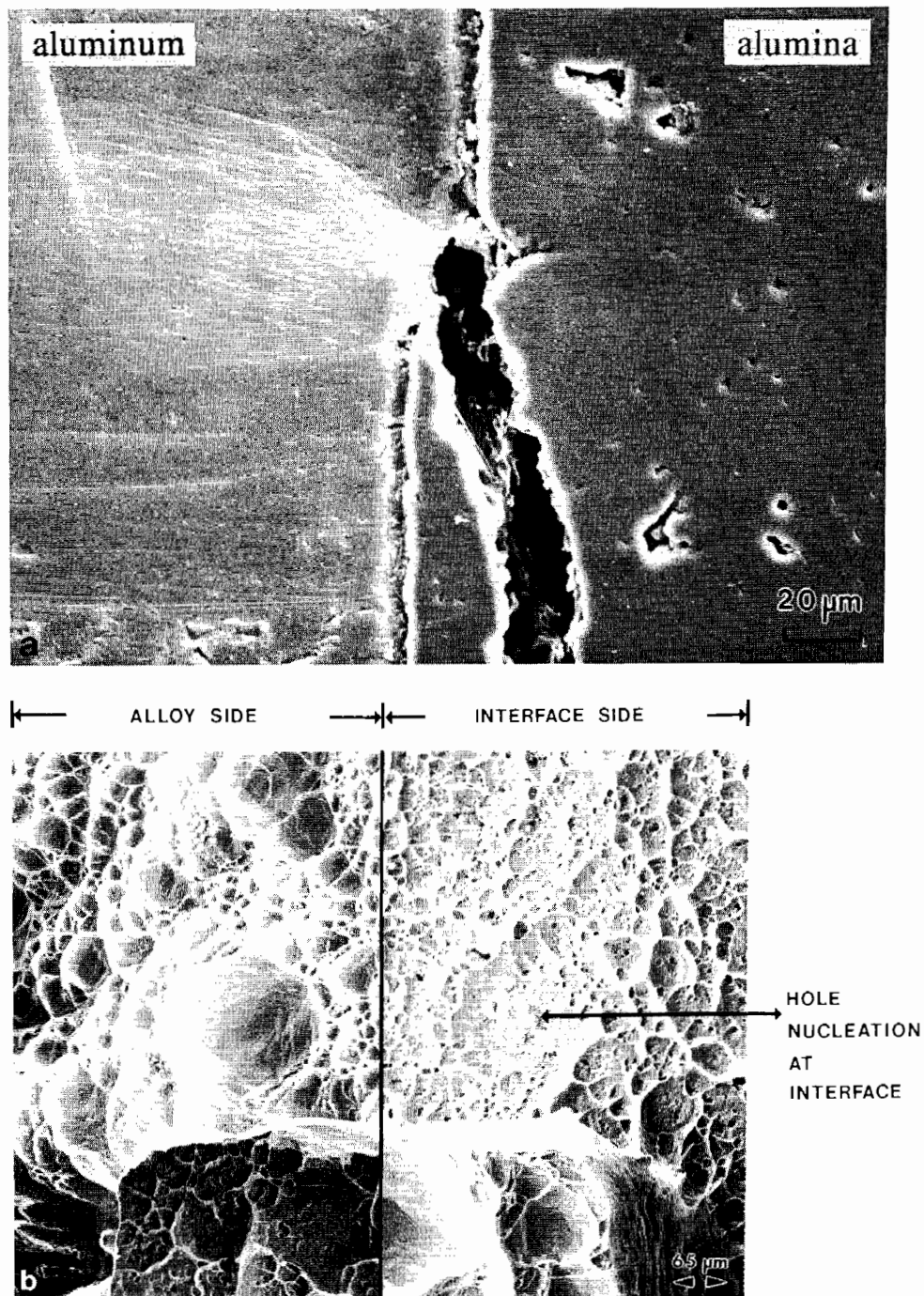


Fig. 6. (a) Plastic blunting at the interface: a crack in the Al<sub>2</sub>O<sub>3</sub>/Al system. (b) Ductile fracture surface: failure adjacent to the interface in the Al<sub>2</sub>O<sub>3</sub>/Al system.

Bond layers having a lower thermal expansion coefficient invariably generate a phase angle that diverts cracks toward the interface. Then, the measured fracture energy can either be larger or smaller than  $\Gamma_s$ , depending upon the residual strain contribution to  $G$ , the influence of plasticity, roughness, etc.

### 3.2. Film decohesion

Films and coatings with interface edge cracks that

cause decohesion experience mixed mode conditions, with  $\psi$  dependent largely on the sign of the residual stress [17]. Films in tension give  $\psi \approx 45^\circ$  with sign that tends to deflect the crack away from the interface. Consequently, when the substrate is brittle and the interface fracture energy is relatively high, the decohesion process proceeds in the substrate by cracking at a characteristic depth beneath the interface [9–11]. The substrate fracture energy  $\Gamma_s$  then

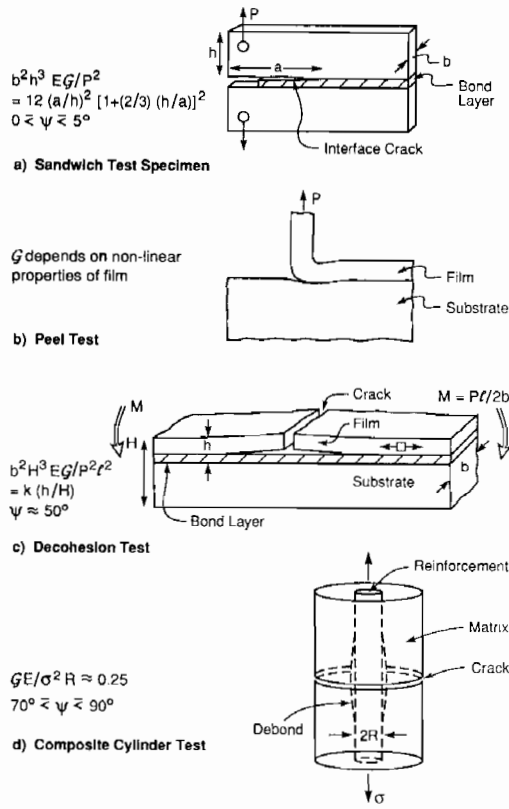


Fig. 7. A schematic indicating the various tests used to measure the interface fracture energy.

becomes the relevant quantity. When the substrate is ductile, the incidence of decohesion is governed by  $\Gamma_i$ , which may be influenced by plasticity in

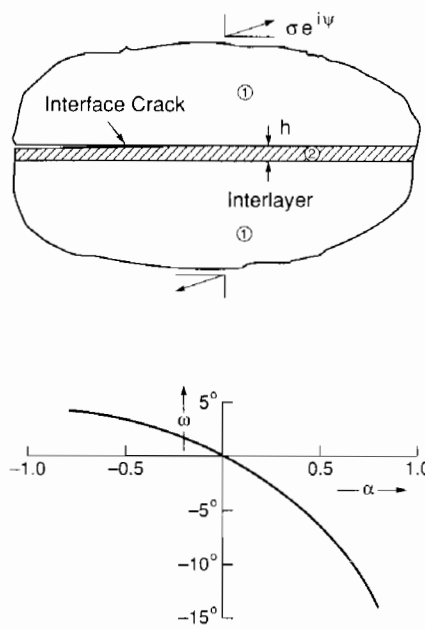


Fig. 8. The phase angle shift  $\omega$  for a sandwich specimen as a function of the elastic mismatch across the interface, expressed through the Dundurs' parameter  $\alpha$ .

the substrate, etc. When decohesion does occur at the interface (Fig. 9), the decohesion analysis [11] may be used to measure  $\Gamma_i$ .

Residual compression in the film subjects edge cracks to mode II conditions, plus compression normal to the interface. As yet, there is no understanding of interface fracture in such circumstances.

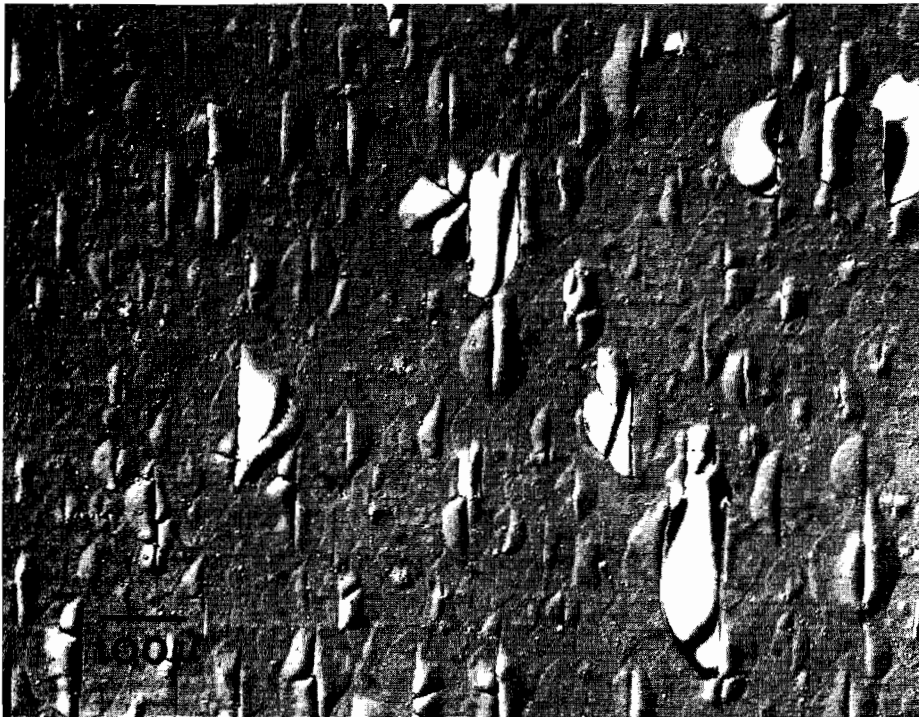


Fig. 9. Film cracking followed by interface decohesion for Cr films deposited onto stainless steel.

### 3.3. Peel tests

The peel test is generally used for measuring the fracture energy of ductile compliant films on substrates [5]. The phase angle has a negative sign that causes substrate cracks to deviate into the interface. The test thus encourages the modes of interface fracture depicted on the left side of Fig. 6. The measured fracture energy can be appreciably less than the substrate value  $\Gamma_s$ , and include contributions from crack tip plasticity in the film material. One complication with this test is that the peel load is sensitive to non-linear deformation *in the film*, such that deconvolution to obtain  $\Gamma_i$  requires knowledge of the plastic flow stress of the film [5]. However, when this effect is taken into account, valid  $\Gamma_i$  measurements are certainly possible and indeed, can be large compared with  $\Gamma_s$ .

### 4. CONCLUDING REMARKS

A rational mechanics basis for predicting and interpreting crack trajectories in bimaterial systems has been proposed, based on knowledge of the phase angle of loading,  $\psi$ . In particular, the sign and magnitude of  $\psi$  dictate whether cracks either propagate along an interface or deviate into the adjoining material and extend parallel to the interface. More importantly, phase angle conditions that motivate cracks to remain at the interface can, in some cases, yield interface fracture energies  $\Gamma_i$  in excess of that for the brittle member *even though the crack propagates at the interface*. Such high fracture energies contain contributions from plasticity, roughness-induced crack shielding, etc.

The phase angle of loading is strongly influenced by the choice of test specimen and thus,  $\Gamma_i$  experimentally determined on the same bimaterial interface can vary appreciably between test specimens. However, it is believed that a unique relationship exists between  $\Gamma_i$  and  $\psi$  for a given interface. It is thus emphasized that test specimens *must* be characterized *both* in terms of an *energy release rate* and a *phase angle of loading*. As more data on  $\Gamma_i(\psi)$  are generated, the

mechanisms that contribute to  $\Gamma_i$  can be addressed, and allow the development of a fundamental evaluation of interface fracture.

An important corollary of the above conclusion is that the prediction of such events as fiber debonding in composites, film decohesion and bond fracture require that *both*  $G$  and  $\psi$  be evaluated for the problem. Then, provided that  $\Gamma_i$  has been measured in the appropriate range of  $\psi$ , prediction can be made. This point is emphasized because  $\psi$  is typically much more difficult to calculate than  $G$ , and its evaluation is essential if interface cracking problems are to be adequately understood. Furthermore, schemes for calculating  $\psi$  using either integral equations or finite elements have been developed.

### REFERENCES

1. B. J. Dalgleish, M. C. Lu and A. G. Evans, *Acta metall.* **36**, 2029 (1988).
2. K. Burger, D. Brenner and G. Petzow, *Z. Zahn. Implant.* **III**, 547 (1987).
3. B. J. Dalgleish, K. P. Trumble and A. G. Evans, *Acta metall.* **37**, 1923 (1989).
4. T. S. Oh, J. Rödel, R. O. Ritchie and R. M. Cannon, *Acta metall.*, **36**, 2083 (1988).
5. K. S. Kim and N. Aravas, *Int. J. Solids Struct.* **24**, 417 (1988).
6. R. F. Pabst and G. Elssner, *J. Mater. Sci.* **15**, 188 (1980).
7. M. He and J. W. Hutchinson, *J. appl. Mech.* **56**, 270 (1989).
8. M. D. Thouless, A. G. Evans, M. F. Ashby and J. W. Hutchinson, *Acta metall.* **35**, 1333 (1987).
9. M. S. Hu, M. D. Thouless and A. G. Evans, *Acta metall.* **36**, 1301 (1988).
10. M. D. Drory and A. G. Evans, *J. Am. Ceram. Soc.* Submitted.
11. Z. Suo and J. W. Hutchinson, *Int. J. Solids Struct.* In press.
12. J. R. Rice, *J. appl. Mech.* **55**, 98 (1988).
13. Z. Suo and J. W. Hutchinson, *Mater. Sci. Engng A* **107**, 135 (1989).
14. M. S. Hu and A. G. Evans, *Acta metall.* **37**, 917 (1989).
15. H. C. Cao, M. D. Thouless and A. G. Evans, *Acta metall.* **36**, 2037 (1988).
16. H. P. Kirchner, J. C. Conway and A. E. Segall, *Jl. Am. Ceram. Soc.* **70**, 104 (1987).
17. Z. Suo and J. W. Hutchinson, *Int. J. Fract.* In press.